1	Title: Non-destructive spatial analysis of phosphatase activity and total protein distribution in the
2	rhizosphere using a root blotting method
3	
4	Authors: Vivian S. Lin <sup>1</sup> , Joshua J. Rosnow <sup>1</sup> , Monee Y. McGrady <sup>1</sup> , Darian N. Smercina <sup>2</sup> , Jamie
5	Nuñez <sup>1</sup> , Ryan S. Renslow <sup>1</sup> , James J. Moran <sup>3</sup> *
6	
7	<sup>1</sup> Biological Sciences Division, Pacific Northwest National Laboratory, Richland, Washington
8	99354, United States
9	<sup>2</sup> Department of Plant, Soil and Microbial Sciences, Michigan State University, East Lansing, MI
LO	48823, United States
11	<sup>3</sup> Environmental Molecular Sciences Laboratory, Pacific Northwest National Laboratory,
12	Richland, WA 99354, United States
L3	*Corresponding author: <u>James.Moran@pnnl.gov</u> ; Pacific National Laboratory, P.O. Box 999,
L4	MSIN K8-91, Richland, WA 99352 USA
<b>L</b> 5	
L6	Declaration of interest: none.
L <b>7</b>	
L8	Abstract
L9	Phosphorus (P) is an essential macronutrient for plant growth, but bioavailable P in soils
20	is often limited due to immobilization resulting from pH and geochemical interactions.
21	Understanding the dynamics of P in soils and elucidating the mechanisms by which plants access
22	P from their environment are critical to evaluating productivity, particularly in nutrient poor
23	environments. Phosphorus from organic matter can act as a major source of P for organisms in

soil systems. Phosphatases, enzymes that liberate inorganic P from organic sources, are produced
by both plants and microbes and are considered one of the most active classes of enzymes in soil.
We developed a root blotting method to spatially image phosphatase activity in the rhizosphere.
Proteins from the rhizosphere are transferred to a nitrocellulose membrane while retaining their
enzymatic activity and two-dimensional spatial distribution. Subsequent application of a
fluorogenic phosphatase indicator, DDAO phosphate, enables visualization of the distribution of
phosphatase activity in the sample. The proteins can then be fixed to the membrane and treated
with SYPRO® Ruby Protein Blot Stain, a fluorescent total protein stain, allowing for
visualization of total protein distribution. Taken together, the images of phosphatase activity and
total protein localization can be mapped back to the root architecture and provide insight into
factors affecting the spatial distribution of enzymatic activity and protein accumulation in the
rhizosphere. Notably, this method can be applied to plants growing in rhizoboxes containing soil
or soilless growth mixtures (e.g., sand or various potting mixes) and, because of the non-
destructive nature of this approach, be performed over time to track changes. We anticipate that
this fluorescent indicator imaging technique on root blots can be used in diverse plant-microbe-
soil systems to better understand the role of phosphatases in P acquisition and soil P cycling.

# Keywords

Rhizosphere, root exudates, phosphatase activity, protein localization

# 1. Introduction

Phosphorus (P) is an essential macronutrient for plants, second only to nitrogen in required uptake, and is only bioavailable to plants as inorganic phosphate. However, inorganic

47

48

49

50

51

52

53

54

55

56

57

58

59

60

61

62

63

64

65

66

67

68

phosphate is frequently bound up with calcium, iron, or aluminum minerals and not readily accessible to plants (Hinsinger, 2001; Shen et al., 2011). Low P bioavailability is a major challenge worldwide and P amendments are frequently used to increase crop productivity (Vance, 2001). The majority of commercial P fertilizers are derived from the processing of rock phosphate, which is a nonrenewable resource (Cordell and White, 2011). Furthermore, overapplication of P in agricultural settings has led to significant environmental problems, including eutrophication in major water bodies (Sharpley et al., 1994). Global demand for P is expected to rise as food production increases to feed a growing world population (Cordell et al., 2009; Cordell and White, 2011). Given predictions of a global phosphate shortage in the next 50-100 years (Cordell et al., 2009), approaches to studying P dynamics between plants, microbial communities, and soils are needed to understand the complex mechanisms affecting P acquisition (George et al., 2016; George et al., 2017). Expanding our understanding of P dynamics in the rhizosphere may help us identify potential strategies by which P can be utilized more efficiently in diverse systems. Plants have evolved a variety of strategies to access phosphate from their environment (Hammond et al., 2004; Shen et al., 2011; Hunter et al., 2014). Under phosphate-limiting conditions, many plants modify their root growth architecture to seek out phosphate resources at shallow soil depth (Vance et al., 2003; Peret et al., 2014). Additionally, plants may release organic acids in root exudates to lower the local pH in the rhizosphere, enhancing the solubility of P from mineral sources (Hinsinger, 2001; Richardson et al., 2009). Plants, bacteria, and fungi can also produce phosphatases, which mineralize P from organic P sources, such as organic matter and phytic acid (Dakora and Phillips, 2002; Richardson and Simpson, 2011). While

69

70

71

72

73

74

75

76

77

78

79

80

81

82

83

84

85

86

87

88

89

90

91

organic P is thought to be of particular importance in tropical soils, this may be an underestimated source of P in other ecosystems (Cabugao et al., 2017; Margalef et al., 2017). Phosphatases play a critical role in P cycling and, as a result, are a frequently studied class of enzymes in soil (Caldwell, 2005; Das and Varma, 2011; Nannipieri et al., 2011). Plants primarily produce acid phosphatases (Duff et al., 1994), whereas soil bacteria and fungi possess both acid and alkaline phosphatases that may be released into the environment (Nakas et al., 1987; Dakora and Phillips, 2002). Phosphatase production and the capacity to solubilize phosphate has been used as a key predictor of beneficial plant growth promoting bacteria and fungi (Richardson and Simpson, 2011). The dynamic interplay between soil microbes that convert mineralized P to biologically accessible forms, and the microbes and plants that compete for the nutrient remain elusive, but investigation of the biological mechanisms governing these processes is underway (Shen et al., 2011; Owen et al., 2015). Many enzymatic assays, including phosphatase activity assays, have been applied to bulk soil samples and microbial isolates to assess their biological activity (Marx et al., 2001; Saiya-Cork et al., 2002; Caldwell, 2005; DeForest, 2009; Nannipieri et al., 2011). These approaches are important first steps to evaluating the overall functional potential of specific soil environments. However, given the high spatial heterogeneity of chemical and biological processes occurring at

Soil zymography has been used to spatially examine enzyme activity, with optimization of the materials including various combinations of gel, filter paper, and membranes (Dinkelaker

approaches. To facilitate advanced investigations of interactions occurring between plants and

microbes in soil microenvironments, we developed a membrane blotting approach to capture

pore- and sub-pore scales, additional methods are needed to complement existing bulk

proteins from the rhizosphere and evaluate both their activity and spatial distribution.

and Marschner, 1992; Grierson and Comerford, 2000; Spohn et al., 2013; Spohn and Kuzyakov,		
2014; Guber et al., 2018; Heitkötter and Marschner, 2018; Ma et al., 2018; Nassal et al., 2018).		
Spatially focused investigations of phosphatase activity in the rhizosphere have relied on a		
variety of fluorescent and colorimetric phosphatase indicators, primarily based on		
methylumbelliferone (MUB). Spohn and coworkers utilized MUB phosphate with both gel and		
membrane surfaces to map phosphatase activity in conjunction with carbon allocation in the		
lupine rhizosphere (Spohn and Kuzyakov, 2013). MUB phosphate is commercially available,		
inexpensive, and has been used extensively for phosphatase activity in bulk samples, including		
water and soil (Guilbault et al., 1968; Hoppe, 1993; Freeman et al., 1995; Marx et al., 2001; Bell		
et al., 2013). A wide range of MUB substrates for other enzymes, such as $\beta$ -N-		
acetylglucosaminidase and $\beta$ -glucosidase, are also commercially available. Marschner $\textit{et al.}$ and		
Grierson et al. have applied a similar approach using a two component mixture of naphthol		
phosphate and the diazonium reagent Fast Red TR on filter paper and nitrocellulose membranes,		
respectively, to detect phosphatase activity in the rhizosphere through formation of the red azo		
dye precipitate (Dinkelaker and Marschner, 1992; Grierson and Comerford, 2000). Fast Red TR		
and naphthol phosphate-based reagents provide excellent spatial information as the azo dye		
product is insoluble in water and will not migrate from the site of reaction; however, these		
reagents must be used at relatively high millimolar concentrations and may require several hours		
for development of a visible signal (Dinkelaker and Marschner, 1992).		
In order to expand the existing capabilities for spatially mapping enzyme activity in the		
rhizosphere, we sought an alternative fluorescent substrate with photophysical properties that are		
complementary to other common fluorescent indicators, such as those based on MUB.		
Fluorescein-based substrates, while sufficiently red-shifted from the LIV-excited MLIB, are too		

115

116

117

118

119

120

121

122

123

124

125

126

127

128

129

130

131

132

133

134

135

136

137

water soluble and prone to diffusion to enable spatially resolved analysis. We therefore focused on a different commercially available fluorogenic phosphatase substrate, DDAO phosphate, which has red fluorescence after being activated by either alkaline or acid phosphatases. DDAO phosphate displays good water solubility and turnover rates, making it a promising indicator for imaging phosphatase activity. The resulting fluorescent product, DDAO, is largely water insoluble and does not migrate from the site of activation; DDAO also has an excitation maximum that is shifted over 200 nm from that of DDAO phosphate, resulting in little spectral overlap. This fluorescent probe for phosphatase activity has been applied previously to various biological systems (Leira et al., 2000), although to our knowledge, it has not been reported for use in soil or environmental systems. Applying fluorescent indicators to complex matrices such as soil is challenging due to unexpected interactions of the substrate with diverse, potentially reactive, and often poorly described components (Foster et al., 2018). We, therefore, performed a test to evaluate the extent of unintended fluorescence from this approach by pretreating selected samples with a broad-spectrum phosphatase inhibitor cocktail to evaluate the level of background signal expected when using this method and to confirm that the majority of the fluorescence observed after staining with DDAO phosphate is phosphatase dependent. We also coupled this assay for phosphatase activity with a general protein stain using the commercial reagent SYPRO® Ruby Protein Blot Stain, which provides a measure of the overall amounts of protein transferred to the membrane, akin to a loading control. Dual detection of enzymatic activity and total protein has previously been applied to Western blotting approaches, although these methods are reliant on alkaline phosphatase-conjugated antibodies for signal amplification rather than detection of native enzyme activities in a sample (Top et al., 2001).

High amounts of labile proteins produced in the rhizosphere may be indicative of soil hotspots,

or localized regions where nutrient exchange and biological interactions and activities are highly concentrated (Kuzyakov and Blagodatskaya, 2015). By mapping the spatial distribution of these protein hotspots with phosphatase activity, we can begin to examine the spatial focusing of specific biological activities in the rhizosphere toward heterogeneously distributed nutrients in the soil.

We present the application of a non-destructive root blotting method involving the application of nitrocellulose membrane to the soil and root interface, enabling capture of proteins on the membrane surface and subsequent analysis using fluorogenic reagents to determine the distribution of phosphatase activity and total protein content (Figure 1). This method can be used in soil systems as well as various synthetic plant growth mixtures (e.g., sand or different potting mix formulas). Furthermore, we have developed an open-source image analysis module to quantify spatial differences in root blot images. We highlight the application of the enzyme assay and use of our image analysis method for linking enzyme activity distribution to root architecture by imposing heterogeneous amendment of nutrient resources in rhizobox soil and track the resulting phosphatase spatial distribution in the system.

### 2. Materials and Methods

# 2.1 Seed sterilization

To avoid undesired microbial growth in the sand-filled rhizoboxes (see section 2.2), switchgrass seeds for sand rhizobox experiments were surface-sterilized according to the following procedure. 'Cave-in-Rock' switchgrass seeds from Native Connections (Three Rivers, Michigan, USA) were acid scarified for 5 min in 8 M sulfuric acid with agitation. Seeds were washed with

3 x 5 min of deionized water, drained thoroughly, and then imbibed on Whatman #1 filter paper with 5 mL of sterile 0.2% (m/v) KNO<sub>3</sub> at 4 °C for 7 days. Seeds were then bleach sterilized with 3 x 5 min exchanges of 5% Clorox® bleach with agitation, rinsed thoroughly with 3 x 5 min deionized water, and spread into a single layer in a Petri dish using a spatula. The Petri dish was placed in a glass desiccator inside a fume hood. Seeds were then exposed to chlorine gas, generated by the addition of 3 mL concentrated hydrochloric acid to 100 mL Clorox® bleach in a 250 mL beaker. The desiccator was immediately sealed and allowed to stand for 4 hr. After sterilization, the desiccator was opened and allowed to vent inside the fume hood for 1 hr. The Petri dish was covered, sealed with parafilm, and stored at 4 °C, protected from light.

2.2 Plant growth and imaging in sand-filled rhizobox

40-100 mesh sand (Acros) was combusted at 500 °C for 8 hr. To avoid microbial contamination, all materials for rhizobox assembly were autoclaved at 121 °C, 15 psi for 30 min and non-autoclavable supplies were sterilized with 70% ethanol and 30 min of exposure to UV light in a laminar flow hood. Sterilized switchgrass seeds were germinated in sterile 1% potassium nitrate solution in glass beads and incubated in the dark at 28 °C for 6-11 days before planting in sand.

Rhizobox assembly and opening of jars were performed in a laminar flow hood. Empty

Lexan rhizoboxes (7.6 cm x 13.3 cm x 3.2 cm; 6 mm wide walls, 2 mm wide front panel) with 10

drainage holes in the bottom were assembled by securing the removable front panel of the

rhizobox with electrical tape and placing a piece of nylon mesh, cut to size, in the bottom of the

box to prevent loss of sand through drainage holes. Rhizoboxes were wrapped around the sides

with aluminum foil to protect the roots from light exposure and placed in 1-gallon glass jars over

a 3-4 cm deep layer of marbles with 100 mL water. Jars were covered with screw-on metal lids (110 mm diameter) in which 8 x 1 cm holes were drilled. Aluminum foil was wrapped over jar lids, and the jars were autoclaved for 30 min at 121 °C, 15 psi in an autoclave-safe plastic bin with 3 inches of water to facilitate even heating of the glass. Once cooled, sterilized jars were transferred to a laminar flow cabinet and jar lid holes were sealed with Breathe-Easy® sealing membranes (Research Products International Corp) to allow for gas exchange. Rhizoboxes were removed from the jars and filled with combusted sand (approximately 160 g per box). Sand rhizoboxes were bottom watered with 40 mL half-strength Hoagland's solution without phosphate (Jiang et al., 2017), the sand was stirred with a spatula to reduce compaction, and seedlings were planted in sand against the front removable panel of the rhizobox with sterile tweezers. Rhizoboxes were placed inside jars at an angle (~45°) to encourage root growth along the front panel of the rhizobox. Sealed jars were then transferred to a reach-in Conviron growth chamber on a 16 hr day/8 hr night cycle, 28 °C, 60% relative humidity. Plants were watered with 1 mL half-strength –P Hoagland's solution on day 7, 5 mL Milli-Q® water on day 20, and 10-15 mL Milli-Q® water on day 30.

Nitrocellulose membranes were autoclaved at 121 °C, 15 psi for 30 min to sterilize and prewetted in autoclaved Milli-Q® water. Membranes were then placed directly onto the sand/root surface. The front panels of the Lexan rhizoboxes were secured with electrical tape, rhizoboxes were wrapped with aluminum foil to protect from light, and plants were returned to their sterile jars. After the set incubation time of membranes against the sand/root surface had passed, membrane blots were removed using tweezers for immediate processing using the described methods for DDAO phosphate and SYPRO® Ruby blot staining. After membrane removal, the rhizobox front panel was replaced, secured with tape, and roots were imaged using

the Typhoon laser scanner. Plants were then returned to their jars until the next root blotting timepoint.

2.3 Plant growth and imaging in soil-filled rhizobox

'Cave-in-Rock' switchgrass (*Panicum virgatum* L., PI 469228) were obtained from the United States Department of Agriculture Agricultural Research Service (USDA-ARS) U.S. National Plant Germplasm System (NPGS) for soil experiments. Seeds were germinated in glass Petri dishes with glass beads in Milli-Q® water and transferred to soil after 7-10 days.

Soil from Kellogg Biological Station (Michigan, USA) was collected in January 2018 and stored at 4 °C in the dark. Soil was sieved through a 4 mm plastic sieve to remove large roots and leaves and then semi-dried in a fume hood for 24 hr. Black high-density polyethylene (HDPE) rhizoboxes (15.2 cm x 20.3 cm x 0.95 cm) with removable clear plexiglass side panels (15.2 cm x 20.3 cm) were dry packed with soil by packing open-face and then filling from the top to reduce soil compaction. Clear side panels were covered with opaque black HDPE side covers (15.2 cm x 20.3 cm) to protect roots from light. Plants were grown in a Conviron walk-in growth chamber (model no. GR48) on a 16 hr light, 8 hr dark cycle, at 24 °C with 50% humidity during the day and 18 °C with 40% humidity at night. Plants were watered every 2-3 days from the top with deionized water.

Roots were blotted at 6 to 11 weeks after planting in soil. For soil rhizoboxes, nitrocellulose membranes were prewetted with deionized water and placed on the soil and root surface. The rhizoboxes were reassembled with the plexiglass panels held in place with screws, and the rhizobox was returned to the growth chamber for 24-72 hr. Membranes were removed and processed as described below for DDAO phosphate and SYPRO® Ruby staining.

Membranes treated with phosphatase inhibitor cocktail were prepared as described for the dot blot assay in the Supporting Information.

# 2.4 DDAO phosphate and SYPRO® Ruby blot staining

Stock solutions of 9H-(1,3-Dichloro-9,9-dimethylacridin-2-one-7-yl) phosphate, diammonium salt (DDAO phosphate, Invitrogen) were prepared by dissolving 5 mg solid probe in Milli-Q® water to a concentration of 5 mM and storing as aliquots at -70 °C, protected from light and avoiding freeze-thaw cycles. DDAO phosphate working solutions were prepared by diluting stock solutions to 10 μM in 50 mM Tris-HCl buffer, pH 6.5. This pH was selected based on previous reports for combined acid and alkaline phosphatase activity measurements (Schurr and Yagil, 1971; Fraser et al., 2017). A dot blot assay was used to confirm both acid and alkaline assays were active at this pH (Figure S1) (Allis et al., 1986). For phosphatase inhibitor experiments, Phosphatase Inhibitor Cocktail 2 (P5726, Sigma Aldrich) was diluted 1:100 in 50 mM Tris-HCl buffer, pH 6.5 and applied to membranes for 10 min prior to DDAO staining.

(typically < 50 cm²) and handled with tweezers to avoid contaminating the exposed membrane surface. Membranes were stained for phosphatase activity by immersing completely in 10 μM DDAO phosphate solution for 5-10 seconds, blotting excess liquid from the corners of the membrane with a Kimwipe<sup>TM</sup> or paper towel, and allowing the membrane to dry fully in air, protected from light. Contact of the wet membrane with surfaces, which will produce artifacts in the staining, was avoided by leaning membranes at an angle or by suspending from one edge using a binder clip during the drying process. Stained membranes were then imaged using the Typhoon laser scanner.

SYPRO <sup>TM</sup> Ruby Protein Blot Stain (Thermo Fisher Scientific) was used according to the
manufacturer's instructions for all staining. Briefly, nitrocellulose membrane blots were fixed in
10% methanol, 7% acetic acid in water for 15 min, as recommended by the manufacturer. The
membranes were washed with 4 x 5 min exchanges of deionized water, stained with SYPRO®
Ruby Protein Blot Stain for 15 min, and rinsed with 6 x 1 min deionized water. Membranes were
then dried in air, protected from light, before imaging with the Typhoon laser scanner.

# 2.5 Instrumentation and membrane imaging

Fluorescence imaging was performed using a Typhoon<sup>TM</sup> FL 9500 laser scanner (GE Healthcare Bio-Sciences AB). Switchgrass (*Panicum* virgatum, var. Cave-in-Rock) roots or membrane blots were imaged at 50 µm resolution using the DDAO phosphate, SYPRO® Ruby, or Alexa Fluor® 488 settings for phosphatase activity, total protein, or root architecture imaging, respectively. Blots were imaged using the same gain settings and processed identically when comparing samples.

# 2.6 Resource island experiment

Organic matter pellets were prepared from freeze-dried (at least 24 hours) annual ryegrass roots. Root material was ground with a mortar and pestle to a homogenous powder. Approximately 0.5 - 0.7 mL of powder was compressed at >2000 psi in a hydraulic press to form a pellet. Pellets were sliced into 6 fractions, approximately 6 mm x 4 mm dimensions (125 mm<sup>2</sup> area), similar in size to quartz chips used as controls. Quartz chips (SiO<sub>2</sub>, quartz turnings from Costech Analytical Technologies, Inc.) were used with no further processing.

Switchgrass seeds were germinated as described above and transferred to rhizoboxes packed with soil from Kellogg Biological Station. Resource islands were placed in rhizoboxes 9-10 days after switchgrass seedlings were introduced to soil and before the roots had reached the depth at which the resource islands were installed. Membrane blotting experiments were performed 34-35 days after resource island placement. Nitrocellulose membranes were placed in rhizoboxes for approximately 48 hr.

# 2.7 Imaging analysis methods

To analyze the levels of phosphatase in the roots and surrounding soil, an open-source Python module, "resource-islands", was developed (<a href="https://github.com/pnnl/rhizo\_phosph">https://github.com/pnnl/rhizo\_phosph</a>) for use on DDAO stained images. Similar to our previous image analysis pipelines for soils (Ilhardt et al., 2019), this module was built using Python (v 3.7.3), with packages opency (v 4.1.0) (Bradski, 2000), matplotlib (v 3.0.3) (Hunter, 2007), numpy (v 1.16.2) (Walt et al., 2011), and seaborn (v 0.9.0) (Waskom et al., 2018), and was implemented using Jupyter Notebook (v 4.4.0) (Kluyver et al., 2016), an interactive Python environment, to create figures and analyze data.

Prior to image analysis, DDAO images were aligned to the camera image using the affine transform function in *opencv*. These images were then cropped to separate the two roots and their corresponding rhizospheres (designated root R1 and root R2 images) for individual analysis, and masks were manually added to the image based on visual identification of the boundary between the root edge and adjacent rhizosphere and we used the masks to differentiate between root and rhizosphere regions (which further included demarcation and masking of soil, organic material pellets, and quartz). Root that is not visible between pieces of visible root were assumed to be covered by a thin layer of soil; these regions were masked by making connections between root

segments that were well defined and very close. Root R1 contained the root section near the organic matter pellet resource islands and associated connected root sections and rhizosphere. Root R2 contained pieces of quartz, the root growing next to them, and the associated rhizosphere. Cropping was done to ensure that organic matter and neighboring regions were not visible in root R2 image, and likewise, no quartz was visible in root R2 image. Because the root in the root R2 image was longer than the root in the R1 image, the R2 image was cropped vertically to match the length of root R1 to enable a fair statistical comparison (i.e., quantitation of data for the same length and root depths). See Figure 5 for final masking, processing, and R1 and R2 demarcation. For all plots, distance was converted from pixels to mm using the conversion 1 pixel = 0.05 mm.

For average pixel intensity figures, averages were calculated separately for root masks and rhizosphere masks. To quantify rhizosphere phosphatase levels, the pixel intensities for soil pixels located 0 to 2 mm on either side of the root were averaged into one value, starting from the top of the image (i.e., top of the root) and going down one row of pixels at a time (Figure S3). Similarly, to quantify average pixel intensity of the root masks themselves, each row of root pixel intensities was averaged into a single value, starting from the top of the image and going down one row of pixels at a time (Figure S8).

Due to the different number of pixels available in the R1 and R2 images, both 1D and 2D histograms were normalized to have a total summed signal of 1. Fitted Gaussian functions were overlaid on each 1D histogram to more easily compare the pixel distributions (Figure S6, Figure S10). Parameters for these curves were calculated using *numpy*.

### 3. Results

To validate our method, we first performed a dot blot assay to confirm purified phosphatase enzymes retained their activity when applied to the membrane. Detection of calf intestinal alkaline phosphatase and wheat germ acid phosphatase activity on nitrocellulose membranes was successful at varying concentrations, while the negative control protein BSA, which lacks phosphatase activity, showed minimal staining from DDAO phosphate (Figure S1). Notably, preventing the membrane from drying out during the course of the experiment was important for maintaining enzymatic activity. This assay also demonstrated that DDAO phosphate can be used to detect both alkaline and acid phosphatase activity under the tested conditions. Loading of proteins onto the membrane was determined by a subsequent SYPRO® Ruby blot stain.

Switchgrass seedlings grown in sand and hydroponic solution were used to demonstrate the blotting method in an axenic live plant rhizosphere system. The developed method allowed for repeated, facile sampling of the rhizosphere at various stages of plant growth. Membrane blotting is non-destructive and can be performed several times on the same sample. For 50 cm<sup>2</sup> membranes, all sample processing and imaging could be performed in under 1.5 hr; significantly larger membranes required longer drying times prior to imaging. In an example of repeated, time-resolved sampling, we observed both total protein and phosphatase distribution being more focused along a primary root at day 21 with an example of increased focusing at the lateral root tips in samples taken at day 27 of growth in a switchgrass seedling (Figure 3). Phosphatase distribution was visually correlated with total protein, as determined using the SYPRO® Ruby Protein Blot Stain, indicating the plants focus both root exudation of proteins and production of active phosphatases at the root tips.

Next, we demonstrated this method could be applied successfully to plant roots growing

in soil. Application of membrane to the root and soil surface of switchgrass plants growing in Kellogg Biological Station soil produced DDAO phosphate images with similar localization of phosphatase activity hotspots around the root tips of branching lateral roots, as well as along much of the primary root (Figure 4). To validate the signal observed from the DDAO phosphate staining was due to phosphatase activity, we treated the membrane with a commercially available phosphatase inhibitor cocktail that inhibits both acid and alkaline phosphatases. Staining of the inhibitor-treated membrane followed by imaging showed reduced levels of fluorescence from DDAO phosphate, while total protein distribution as determined using the SYPRO® Ruby Protein Blot Stain was similar to the previous blot (Figure 4E and 4F). This indicated that the signal from DDAO phosphate can be primarily attributed to phosphatase activity in these rhizosphere samples from switchgrass grown in soil. The remaining signal after inhibitor pretreatment may be a result of nonspecific activation of DDAO phosphate or due to phosphatases that are not inactivated by any of the components in the commercial inhibitor cocktail.

Following successful application of our method to switchgrass plants grown in soil, we sought to examine the distribution of phosphatase activity in the rhizosphere when organic matter resource islands, containing organic phosphorus, were located adjacent to growing roots. Organic matter pellets from root biomass and quartz chips as controls were placed in rhizoboxes, and switchgrass seedlings were allowed to grow toward them (Figure 5). We developed an image analysis method to map phosphatase activity in the switchgrass rhizosphere relative to organic matter pellets or quartz chip controls. Organic matter pellets, quartz chips, and roots were masked by hand (Figure 5). The intensity of the DDAO phosphate stain was quantified for the

root itself and through 2 mm of the adjacent rhizosphere. Quantitative analysis of the DDAO phosphate images showed that fluorescence intensity was increased in the rhizosphere of root R1, which was adjacent to organic matter resource islands, compared to root R2, which was adjacent to inert quartz chip controls (Figure 6); this difference was statistically significant (Welch's test). Additional studies are needed to further explore the influence of resource islands in soil on phosphatase activity and other enzymes of interest in the rhizosphere.

### 4. Discussion

Rhizosphere interactions between plant hosts, colonizing microbes, and the surrounding soil involve complex biological and chemical dynamics. Elucidating these interactions will improve our understanding of the mechanisms by which plants respond to and acquire nutrients from their environment. We describe the application of a fluorogenic phosphatase substrate, DDAO phosphate, in conjunction with a fluorescent total protein stain, SYPRO® Ruby Protein Blot Stain, for non-destructive sampling and visualization of the spatial distribution of phosphatase activity in the switchgrass rhizosphere. This method allows for comparison of phosphatase activity relative to total protein distribution, while allowing for straightforward mapping of root structure with enzyme and protein distribution.

Overall, the combined phosphatase and total protein staining and imaging can be conducted in less than 1.5 hr using commercially available reagents. Transfer of proteins from the plant root and soil surface to the membrane can be achieved using a wide range of incubation times, although SYPRO® Ruby total protein results were improved at longer incubation times (6-24 hr) compared to shorter time frames (5-10 min) (Figure S15). Notably, background in the DDAO phosphate results were much higher at 48 hr and longer incubation

times in soil, potentially due to microbial colonization of the membrane surface. Removal of the membrane before application of the fluorescent indicators eliminates the possibility of transferring dye or buffer reagents to the soil, allowing the sample to be returned to the growth chamber and reanalyzed at a later stage during the growth cycle. Additionally, this workflow shortens the time required for image development to 10-15 min, compared to 1-4 hr for Fast Red TR/naphthol phosphate reagents when treating membranes after application to roots and soil (Dinkelaker and Marschner, 1992). Micromolar concentrations of the DDAO phosphate fluorogenic substrate can be used while maintaining excellent sensitivity for phosphatese activity, compared to millimolar amounts of Fast Red TR and naphthol phosphate.

Soil zymography is considered an average of the enzymatic activities occurring in the sample during the duration of the experiment. Thus, the time frame for incubation of the soil and roots with the membrane must be selected carefully, depending on the system of interest. Previous work has observed differences in calculated enzyme activities using different phosphatase substrates including p-nitrophenyl phosphate and 4-MUB phosphate, suggesting soil phosphatases may have different affinities for these various indicators and may not necessarily reflect the enzymatic potential of the sample for the native substrates (Caldwell, 2005; Nannipieri et al., 2011). Thus, quantification of phosphatase activity in the rhizosphere using synthetic substrates such as DDAO phosphate should be performed with caution and must be considered a relative measure of functional activity among samples analyzed under similar experimental conditions.

In the development of this method, we observed that maintaining suitable soil moisture content is also an important consideration. Drying of the membrane may result in denaturation of proteins adsorbed to the surface and consequently reduce enzyme activity (Figure S16). On the

contrary, excessive moisture in the substrate may result in diffuse blots (Figure S17); Spohn and coworkers previously observed sharper images when using membrane blotting systems rather than a gel to transfer proteins from the rhizosphere, which was attributed to diffusion of the dye through the medium (Spohn and Kuzyakov, 2013). Presumably, diffusion of enzymes through liquid in soils, such as pore water, may also give rise to diffuse images of enzyme activity.

Our root blotting approach and image analysis methods offer new opportunities to interrogate complex plant, microbe, and soil interactions in a spatial manner. We demonstrated the utility of this method for conducting spatially resolved measurements of biological activity in the switchgrass rhizosphere by mapping phosphatase and total protein distribution from switchgrass plants grown in soil rhizoboxes containing organic matter resource islands. Analysis of DDAO phosphate images of root blots showed that the distribution of phosphatase activity was increased in a root adjacent to the organic matter compared to a control root growing near quartz chips. Organic matter may provide an important source of organic P in certain soil systems, and our approach can be used to evaluate spatial focusing of phosphatase activity and root exudation in the rhizosphere in response to heterogeneously distributed nutrient sources.

Future applications of our approach will allow for investigation of spatially directed plant root and microbial responses toward organic P sources in soil systems. Further studies are underway to explore the impact of heterogeneously distributed nutrients in soil on spatial focusing of enzyme activity in the rhizosphere.

We envision that the method presented here will support future efforts to map phosphatase activity and protein content released from the rhizosphere in relation to P sources (inorganic and organic) in soil. Additionally, the flexibility of this approach provides opportunities to map the distribution of other important enzymes in the rhizosphere including β-

N-acetylglucosaminidase and β-glucosidase for nitrogen and carbon acquisition. Having demonstrated the utility of a DDAO based substrate in this method, we envision potential future applications of multiple probes in a suite of colors for multiplexed imaging of different enzymatic activities in a single sample. Combined with both bulk and spatially resolved methods, this approach will facilitate additional studies to examine the complex relationships between plants and microbial communities and provide deeper insight into the factors that influence P dynamics in the rhizosphere.

# 5. Acknowledgements

We are grateful to Elizabeth Denis and Matthew Peterson for assistance with preparing and growing the plant samples used in these experiments. Development of this method was funded by the US Department of Energy (DOE) Office of Biological and Environmental Research (BER) by the Early Career Research Award program (PI: J. Moran). We are also grateful for support provided by the National Science Foundation (NSF) Long-term Ecological Research Program (DEB 1637653) at the Kellogg Biological Station, and by Michigan State University AgBioResearch. We are grateful to the USDA-ARS National Plant Germplasm System for providing switchgrass seeds.

# 6. References:

Allis, C.D., Chicoine, L.G., Glover, C.V.C., White, E.M., Gorovsky, M.A., 1986. Enzyme activity dot blots: A rapid and convenient assay for acetyltransferase or protein kinase activity immobilized on nitrocellulose. Analytical Biochemistry 159, 58-66.

- Bell, C.W., Fricks, B.E., Rocca, J.D., Steinweg, J.M., McMahon, S.K., Wallenstein, M.D., 2013.
- 459 High-throughput fluorometric measurement of potential soil extracellular enzyme activities. J
- 460 Vis Exp, e50961.
- 461 Bradski, G., 2000. The OpenCV Library. Dr. Dobb's Journal of Software Tools.
- Cabugao, K.G., Timm, C.M., Carrell, A.A., Childs, J., Lu, T.S., Pelletier, D.A., Weston, D.J.,
- Norby, R.J., 2017. Root and Rhizosphere Bacterial Phosphatase Activity Varies with Tree
- Species and Soil Phosphorus Availability in Puerto Rico Tropical Forest. Front Plant Sci 8, 1834.
- 465 Caldwell, B.A., 2005. Enzyme activities as a component of soil biodiversity: A review.
- 466 Pedobiologia 49, 637-644.
- 467 Cordell, D., Drangert, J.-O., White, S., 2009. The story of phosphorus: Global food security and
- 468 food for thought. Global Environmental Change 19, 292-305.
- 469 Cordell, D., White, S., 2011. Peak Phosphorus: Clarifying the Key Issues of a Vigorous Debate
- about Long-Term Phosphorus Security. Sustainability 3, 2027-2049.
- Dakora, F.D., Phillips, D.A., 2002. Root exudates as mediators of mineral acquisition in low-
- 472 nutrient environments. Plant and Soil 245, 35-47.
- Das, S.K., Varma, A., 2011. Role of Enzymes in Maintaining Soil Health, In: Shukla, G., Varma,
- 474 A. (Eds.), Soil Enzymology. Springer Berlin Heidelberg, Berlin, Heidelberg, pp. 25-42.
- DeForest, J.L., 2009. The influence of time, storage temperature, and substrate age on potential
- 476 soil enzyme activity in acidic forest soils using MUB-linked substrates and l-DOPA. Soil
- 477 Biology and Biochemistry 41, 1180-1186.
- Dinkelaker, B., Marschner, H., 1992. In vivo demonstration of acid phosphatase activity in the
- 479 rhizosphere of soil-grown plants. Plant and Soil 144, 199-205.

- Duff, S., Sarath, G., Plaxton, W., 1994. The role of acid phosphatases in plant phosphorus
- 481 metabolism. Physiologia Plantarum 90, 791-800.
- Foster, E.J., Fogle, E.J., Cotrufo, M.F., 2018. Sorption to Biochar Impacts -Glucosidase and
- 483 Phosphatase Enzyme Activities. Agriculture-Basel 8.
- 484 Fraser, T.D., Lynch, D.H., Gaiero, J., Khosla, K., Dunfield, K.E., 2017. Quantification of
- bacterial non-specific acid (phoC) and alkaline (phoD) phosphatase genes in bulk and
- 486 rhizosphere soil from organically managed soybean fields. Applied Soil Ecology 111, 48-56.
- Freeman, C., Liska, G., Ostle, N.J., Jones, S.E., Lock, M.A., 1995. The use of fluorogenic
- substrates for measuring enzyme activity in peatlands. Plant and Soil 175, 147-152.
- 489 George, T.S., Giles, C.D., Menezes-Blackburn, D., Condron, L.M., Gama-Rodrigues, A.C., Jaisi,
- 490 D., Lang, F., Neal, A.L., Stutter, M.I., Almeida, D.S., Bol, R., Cabugao, K.G., Celi, L., Cotner,
- 491 J.B., Feng, G., Goll, D.S., Hallama, M., Krueger, J., Plassard, C., Rosling, A., Darch, T., Fraser,
- 492 T., Giesler, R., Richardson, A.E., Tamburini, F., Shand, C.A., Lumsdon, D.G., Zhang, H.,
- Blackwell, M.S.A., Wearing, C., Mezeli, M.M., Almås, Å.R., Audette, Y., Bertrand, I., Beyhaut,
- 494 E., Boitt, G., Bradshaw, N., Brearley, C.A., Bruulsema, T.W., Ciais, P., Cozzolino, V., Duran,
- 495 P.C., Mora, M.L., de Menezes, A.B., Dodd, R.J., Dunfield, K., Engl, C., Frazão, J.J., Garland,
- 496 G., González Jiménez, J.L., Graca, J., Granger, S.J., Harrison, A.F., Heuck, C., Hou, E.Q.,
- Johnes, P.J., Kaiser, K., Kjær, H.A., Klumpp, E., Lamb, A.L., Macintosh, K.A., Mackay, E.B.,
- 498 McGrath, J., McIntyre, C., McLaren, T., Mészáros, E., Missong, A., Mooshammer, M., Negrón,
- 499 C.P., Nelson, L.A., Pfahler, V., Poblete-Grant, P., Randall, M., Seguel, A., Seth, K., Smith, A.C.,
- 500 Smits, M.M., Sobarzo, J.A., Spohn, M., Tawaraya, K., Tibbett, M., Voroney, P., Wallander, H.,
- Wang, L., Wasaki, J., Haygarth, P.M., 2017. Organic phosphorus in the terrestrial environment: a
- perspective on the state of the art and future priorities. Plant and Soil 427, 191-208.

- 503 George, T.S., Hinsinger, P., Turner, B.L., 2016. Phosphorus in soils and plants facing
- phosphorus scarcity. Plant and Soil 401, 1-6.
- Grierson, P.F., Comerford, N.B., 2000. Non-destructive measurement of acid phosphatase
- activity in the rhizosphere using nitrocellulose membranes and image analysis. Plant and Soil
- 507 218/2, 49-57.
- Guber, A.K., Kravchenko, A.N., Razavi, B.S., Blagodatskaya, E., Kuzyakov, Y., 2018.
- Calibration of 2-D soil zymography for correct analysis of enzyme distribution. European journal
- 510 of soil science 70, 715-726.
- Guilbault, G.G., Sadar, S.H., Glazer, R., Haynes, J., 1968. Umbelliferone Phosphate as a
- 512 Substrate for Acid and Alkaline Phosphatase. Analytical Letters 1, 333-345.
- Hammond, J.P., Broadley, M.R., White, P.J., 2004. Genetic responses to phosphorus deficiency.
- 514 Ann Bot 94, 323-332.
- Heitkötter, J., Marschner, B., 2018. Soil zymography as a powerful tool for exploring hotspots
- and substrate limitation in undisturbed subsoil. Soil Biology and Biochemistry 124, 210-217.
- Hinsinger, P., 2001. Bioavailability of soil inorganic P in the rhizosphere as affected by root-
- 518 induced chemical changes: a review. Plant and Soil 237, 173-195.
- Hoppe, H.G., 1993. Use of fluorogenic model substrates for extracellular enzyme activity (EEA)
- measurement of bacteria. Handbook of methods in aquatic microbial ecology, 423-431.
- Hunter, J.D., 2007. Matplotlib: A 2D Graphics Environment. Computing in Science &
- **522** Engineering 9, 90-95.
- Hunter, P.J., Teakle, G.R., Bending, G.D., 2014. Root traits and microbial community
- 524 interactions in relation to phosphorus availability and acquisition, with particular reference to
- 525 Brassica. Front Plant Sci 5, 27.

- 526 Ilhardt, P.D., Nunez, J.R., Denis, E.H., Rosnow, J.J., Krogstad, E.J., Renslow, R.S., Moran, J.J.,
- 527 2019. High-resolution elemental mapping of the root-rhizosphere-soil continuum using laser-
- 528 induced breakdown spectroscopy (LIBS). Soil Biology & Biochemistry 131, 119-132.
- Jiang, H., Zhang, J., Han, Z., Yang, J., Ge, C., Wu, Q., 2017. Revealing new insights into
- 530 different phosphorus-starving responses between two maize (Zea mays) inbred lines by
- transcriptomic and proteomic studies. Sci Rep 7, 44294.
- Kluyver, T., Ragan-Kelley, B., Pérez, F., Granger, B., Bussonnier, M., Frederic, J., Kelley, K.,
- Hamrick, J., Grout, J., Corlay, S., Ivanov, P., Avila, D., Abdalla, S., Willing, C., Team, J.D.,
- 534 2016. Jupyter Notebooks—a publishing format for reproducible computational workflows,
- Positioning and Power in Academic Publishing: Players, Agents and Agendas. IOS Press.
- Kuzyakov, Y., Blagodatskaya, E., 2015. Microbial hotspots and hot moments in soil: Concept &
- review. Soil Biology and Biochemistry 83, 184-199.
- Leira, F., Vieites, J.M., Vieytes, M.R., Botana, L.M., 2000. Characterization of 9H-(1,3-dichlor-
- 539 9,9-dimethylacridin-2-ona-7-yl)-phosphate (DDAO) as substrate of PP-2A in a fluorimetric
- microplate assay for diarrhetic shellfish toxins (DSP). Toxicon 38, 1833-1844.
- Ma, X., Zarebanadkouki, M., Kuzyakov, Y., Blagodatskaya, E., Pausch, J., Razavi, B.S., 2018.
- 542 Spatial patterns of enzyme activities in the rhizosphere: Effects of root hairs and root radius. Soil
- Biology and Biochemistry 118, 69-78.
- Margalef, O., Sardans, J., Fernandez-Martinez, M., Molowny-Horas, R., Janssens, I.A., Ciais, P.,
- Goll, D., Richter, A., Obersteiner, M., Asensio, D., Penuelas, J., 2017. Global patterns of
- phosphatase activity in natural soils. Sci Rep 7, 1337.
- Marx, M.C., Wood, M., Jarvis, S.C., 2001. A microplate fluorimetric assay for the study of
- enzyme diversity in soils. Soil Biology and Biochemistry 33, 1633-1640.

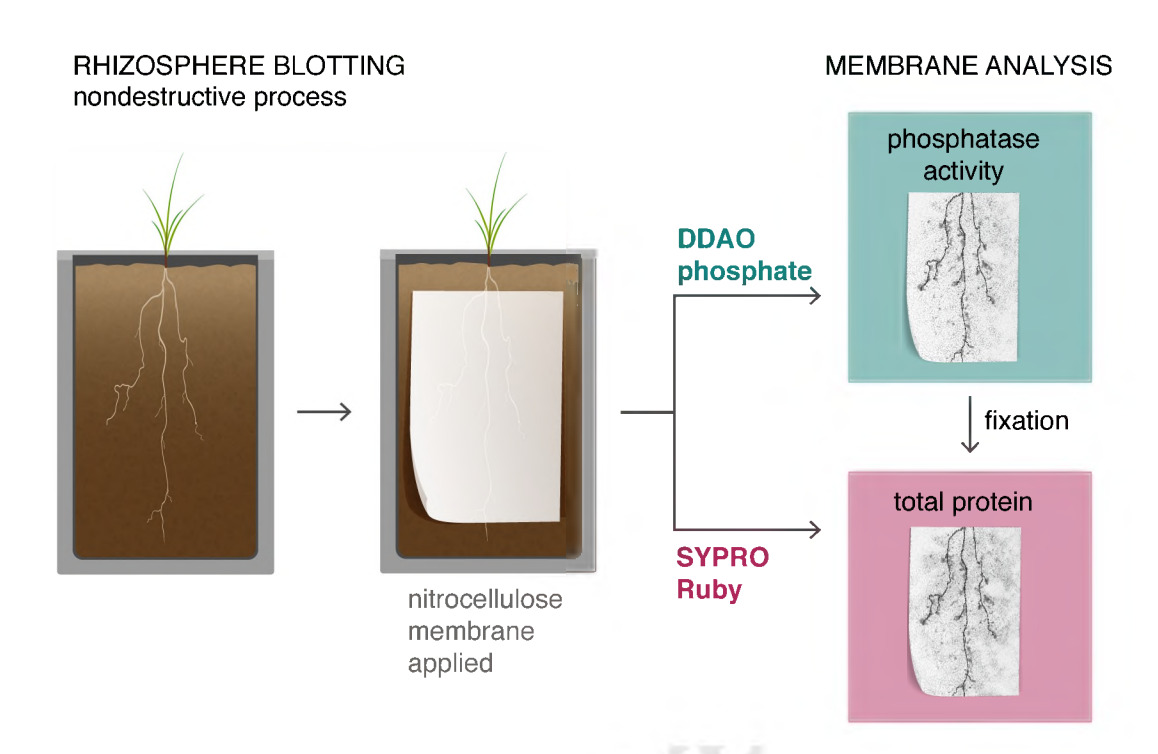
- Nakas, J.P., Gould, W.D., Klein, D.A., 1987. Origin and expression of phosphatase activity in a
- semi-arid grassland soil. Soil Biology and Biochemistry 19, 13-18.
- Nannipieri, P., Giagnoni, L., Landi, L., Renella, G., 2011. Role of Phosphatase Enzymes in Soil,
- In: Bünemann, E., Oberson, A., Frossard, E. (Eds.), Phosphorus in Action: Biological Processes
- in Soil Phosphorus Cycling. Springer Berlin Heidelberg, Berlin, Heidelberg, pp. 215-243.
- Nassal, D., Spohn, M., Eltlbany, N., Jacquiod, S., Smalla, K., Marhan, S., Kandeler, E., 2018.
- Effects of phosphorus-mobilizing bacteria on tomato growth and soil microbial activity. Plant
- 556 and Soil 427, 17-37.
- Owen, D., Williams, A.P., Griffith, G.W., Withers, P.J.A., 2015. Use of commercial bio-
- 558 inoculants to increase agricultural production through improved phosphrous acquisition. Applied
- 559 Soil Ecology 86, 41-54.
- Peret, B., Desnos, T., Jost, R., Kanno, S., Berkowitz, O., Nussaume, L., 2014. Root architecture
- responses: in search of phosphate. Plant Physiol 166, 1713-1723.
- Richardson, A.E., Barea, J.-M., McNeill, A.M., Prigent-Combaret, C., 2009. Acquisition of
- 563 phosphorus and nitrogen in the rhizosphere and plant growth promotion by microorganisms.
- 564 Plant and Soil 321, 305-339.
- Richardson, A.E., Simpson, R.J., 2011. Soil microorganisms mediating phosphorus availability
- update on microbial phosphorus. Plant Physiology 156, 989-996.
- Saiya-Cork, K.R., Sinsabaugh, R.L., Zak, D.R., 2002. The effects of long term nitrogen
- 568 deposition on extracellular enzyme activity in an Acer saccharum forest soil. Soil Biology &
- 569 Biochemistry 34, 1309-1315.
- 570 Schurr, A., Yagil, E., 1971. Regulation and Characterization of Acid and Alkaline Phosphatase
- 571 in Yeast. Journal of General Microbiology 65, 291-&.

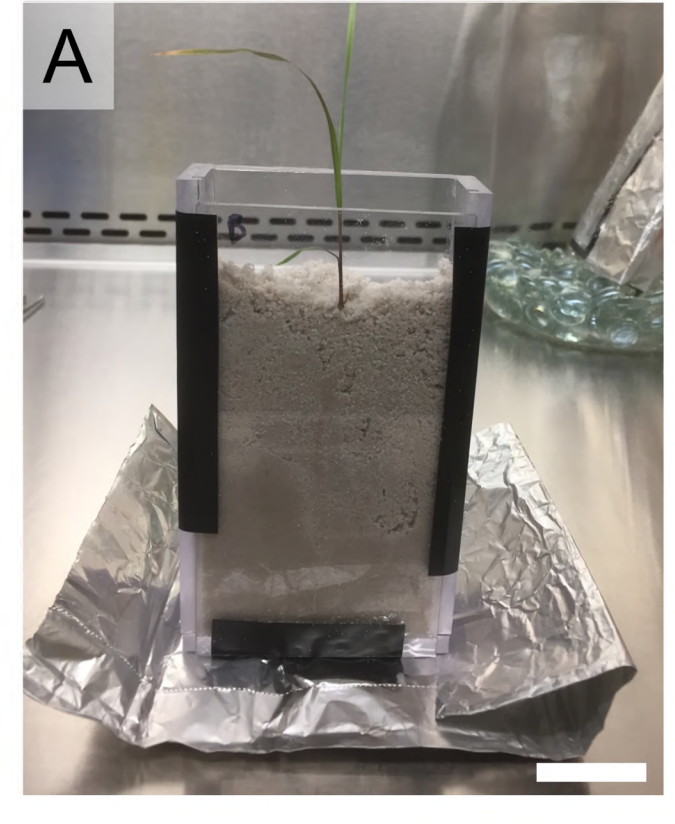
- 572 Sharpley, A.N., Chapra, S.C., Wedepohl, R., Sims, J.T., Daniel, T.C., Reddy, K.R., 1994.
- 573 Managing Agricultural Phosphorus for Protection of Surface Waters: Issues and Options. Journal
- of Environment Quality 23.
- 575 Shen, J., Yuan, L., Zhang, J., Li, H., Bai, Z., Chen, X., Zhang, W., Zhang, F., 2011. Phosphorus
- dynamics: from soil to plant. Plant Physiology 156, 997-1005.
- 577 Spohn, M., Carminati, A., Kuzyakov, Y., 2013. Soil zymography A novel in situ method for
- 578 mapping distribution of enzyme activity in soil. Soil Biology and Biochemistry 58, 275-280.
- 579 Spohn, M., Kuzyakov, Y., 2013. Distribution of microbial- and root-derived phosphatase
- activities in the rhizosphere depending on P availability and C allocation Coupling soil
- zymography with 14C imaging. Soil Biology and Biochemistry 67, 106-113.
- Spohn, M., Kuzyakov, Y., 2014. Spatial and temporal dynamics of hotspots of enzyme activity
- in soil as affected by living and dead roots—a soil zymography analysis. Plant and Soil 379, 67-
- 584 77.
- Top, K.P., Hatleberg, G., Berggren, K.N., Ryan, D., Kemper, C., Haugland, R.P., Patton, W.F.,
- 586 2001. Green/red dual fluorescence detection of total protein and alkaline phosphate-conjugated
- probes on blotting membranes. Electrophoresis 22, 896-905.
- Vance, C.P., 2001. Symbiotic Nitrogen Fixation and Phosphorus Acquisition. Plant Nutrition in a
- World of Declining Renewable Resources. Plant Physiology 127, 390-397.
- Vance, C.P., Uhde-Stone, C., Allan, D.L., 2003. Phosphorus acquisition and use: critical
- adaptations by plants for securing a nonrenewable resource. New Phytologist 157, 423-447.
- Walt, S.v.d., Colbert, S.C., Varoquaux, G., 2011. The NumPy Array: A Structure for Efficient
- Numerical Computation. Computing in Science & Engineering 13, 22-30.

594	Waskom, M., Botvinnik, O., O'Kane, D., Hobson, P., Ostblom, J., Lukauskas, S., Gemperline,
595	D.C., Augspurger, T., Halchenko, Y., Cole, J.B., Warmenhoven, J., Ruiter, J.d., Pye, C., Hoyer,
596	S., Vanderplas, J., Villalba, S., Kunter, G., Quintero, E., Bachant, P., Martin, M., Meyer, K.,
597	Miles, A., Ram, Y., Brunner, T., Yarkoni, T., Williams, M.L., Evans, C., Fitzgerald, C., Brian,
598	Qalieh, A., 2018. mwaskom/seaborn: v0.9.0 (July 2018), Zenodo.
599	
600	
601	Figure captions
602	Figure 1. Schematic of workflow for root blotting using nitrocellulose membrane to capture
603	proteins from the rhizosphere. Switchgrass is grown in a rhizobox with sand or soil matrix.
604	Nitrocellulose membrane is cut to size, prewetted in water, and applied to the soil/root surface.
605	The rhizobox covers are replaced, and the plant is allowed to grow for the specified time after
606	which the membrane is removed and treated with DDAO phosphate, a fluorescent indicator of
607	phosphatase activity. The membrane can then be fixed and stained with SYPRO® Ruby Protein
608	Blot Stain, a fluorescent protein dye. Alternatively, membranes can be fixed and stained with
609	SYPRO® Ruby immediately after collection if phosphatase distribution is not required.
610	Fluorescence imaging of the membrane blots provides a map of rhizosphere phosphatase activity
611	and total protein distribution.
612	
613	Figure 2. Sterile sand rhizobox (A-C) and soil rhizobox (D-F). Rhizoboxes were designed with
614	clear front panels to allow for viewing the root architecture during growth (A, D) and to facilitate

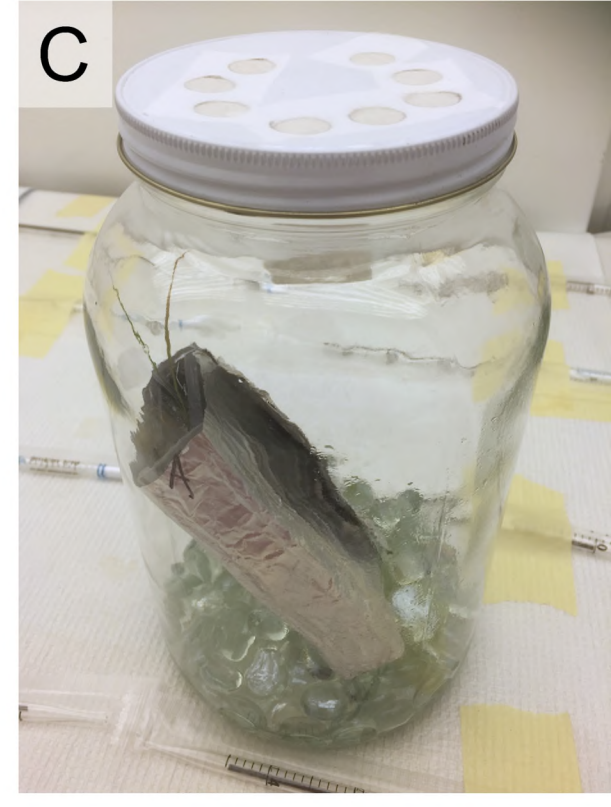
615	placement of membranes (B, E) for sampling proteins in the rhizosphere. Rhizoboxes were
616	oriented at a 45° angle (C, F) to promote root growth along the front panel.
617	Scale bar = 3 cm.
618	
619	Figure 3. Spatial distribution of phosphatase activity and total protein in switchgrass grown in
620	sand at two different timepoints during growth. Plants were supplied with half-strength -P
621	Hoagland's solution. Nitrocellulose membranes were placed against the root/sand surface (D, H)
622	for 24 hr. Spatial distribution of phosphatase activity was determined using DDAO phosphate
623	indicator (A, E). Total protein was stained using SYPRO® Ruby Protein Blot Stain (B, F). Plant
624	roots were imaged directly (C, G) in their rhizoboxes using the Typhoon laser scanner with
625	excitation at 473 nm. Scale bar = 10 mm. Arrows indicate location of selected root tips.
626	
627	Figure 4. Spatial distribution of phosphatase activity and total protein in switchgrass grown in
628	soil from Kellogg Biological Station. Nitrocellulose membranes were placed against the
629	root/sand surface (D, H) for 20-24 hr and imaged for (A, E) spatial distribution of phosphatase
630	activity and total protein (B, F). Plant roots were imaged directly (C, G) within rhizoboxes using
631	excitation at 473 nm. Membranes were treated with a 1:100 dilution of phosphatase inhibitor
632	cocktail (E, F) to confirm DDAO phosphate staining is phosphatase dependent. Scale bar = 10
633	mm.
634	
635	Figure 5. Phosphatase activity in the switchgrass rhizosphere relative to organic matter resource
636	islands and quartz chip controls in soil. (A) A photograph of roots (R1 and R2) originating from
637	a single plant. Original uncropped images are available in the Supporting Information. (B) A

white mask was applied to the root and the organic material or quartz chips were outlined in
black. Places where the root was not visible are outlined and were also masked for analysis. (C)
Corresponding root blot from 48 hr incubation in the soil, stained with DDAO phosphate. (D)
Pixel intensity of DDAO phosphate stain image displayed as a heat map for the rhizosphere,
defined as the area encompassing the root and the adjacent 2 mm of soil.
Figure 6. Image analysis of root blots stained with DDAO phosphate and root images. Average
DDAO abasahata nivel intensity managing the average abasahatase levels of the roots and 2
DDAO phosphate pixel intensity measuring the average phosphatase levels of the roots and 2
mm of soil surrounding the roots. Solid lines represent average pixel intensities and shading
mm of soil surrounding the roots. Solid lines represent average pixel intensities and shading
mm of soil surrounding the roots. Solid lines represent average pixel intensities and shading represents the standard deviation for each row of pixels. Solid black rectangles representing





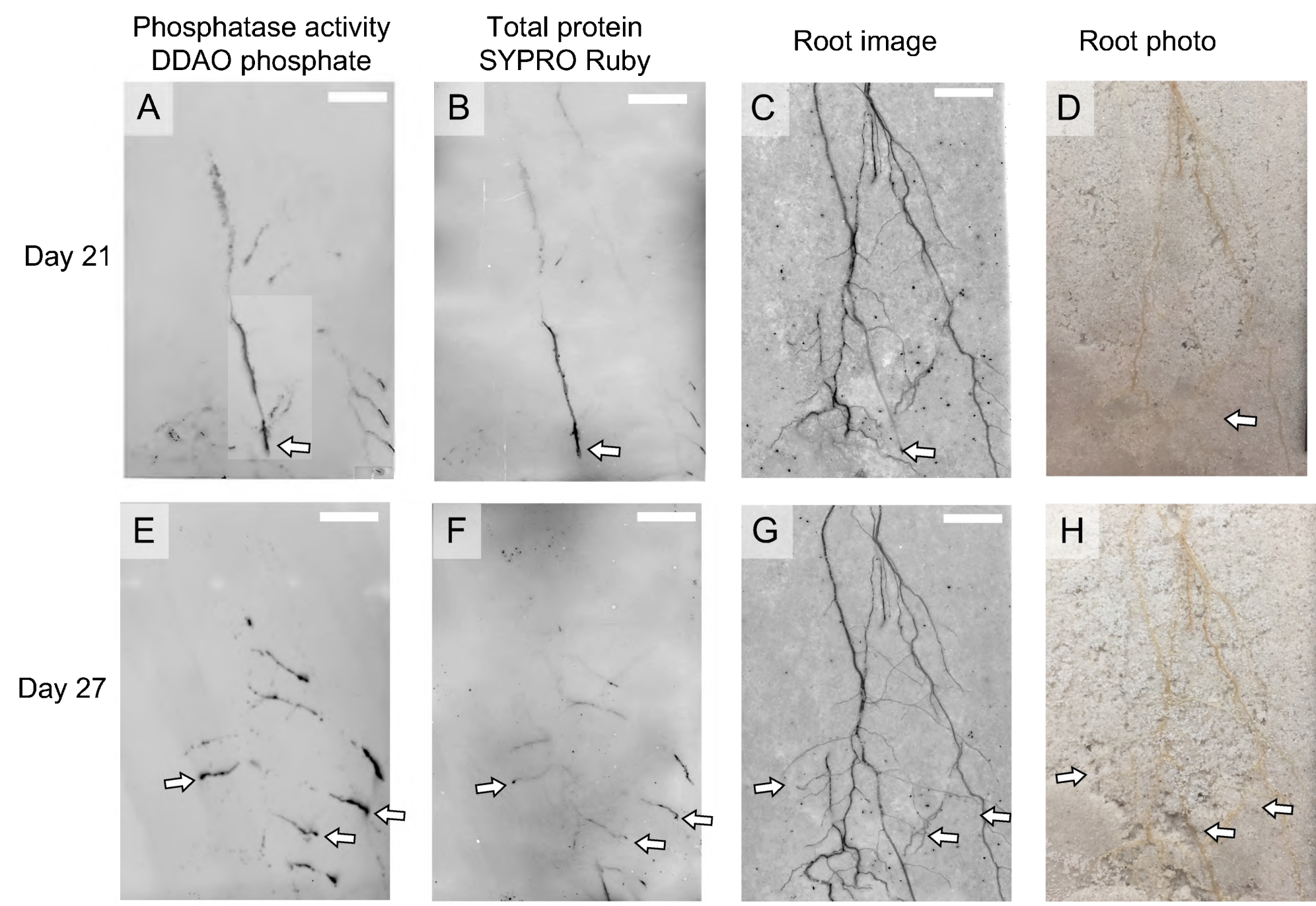


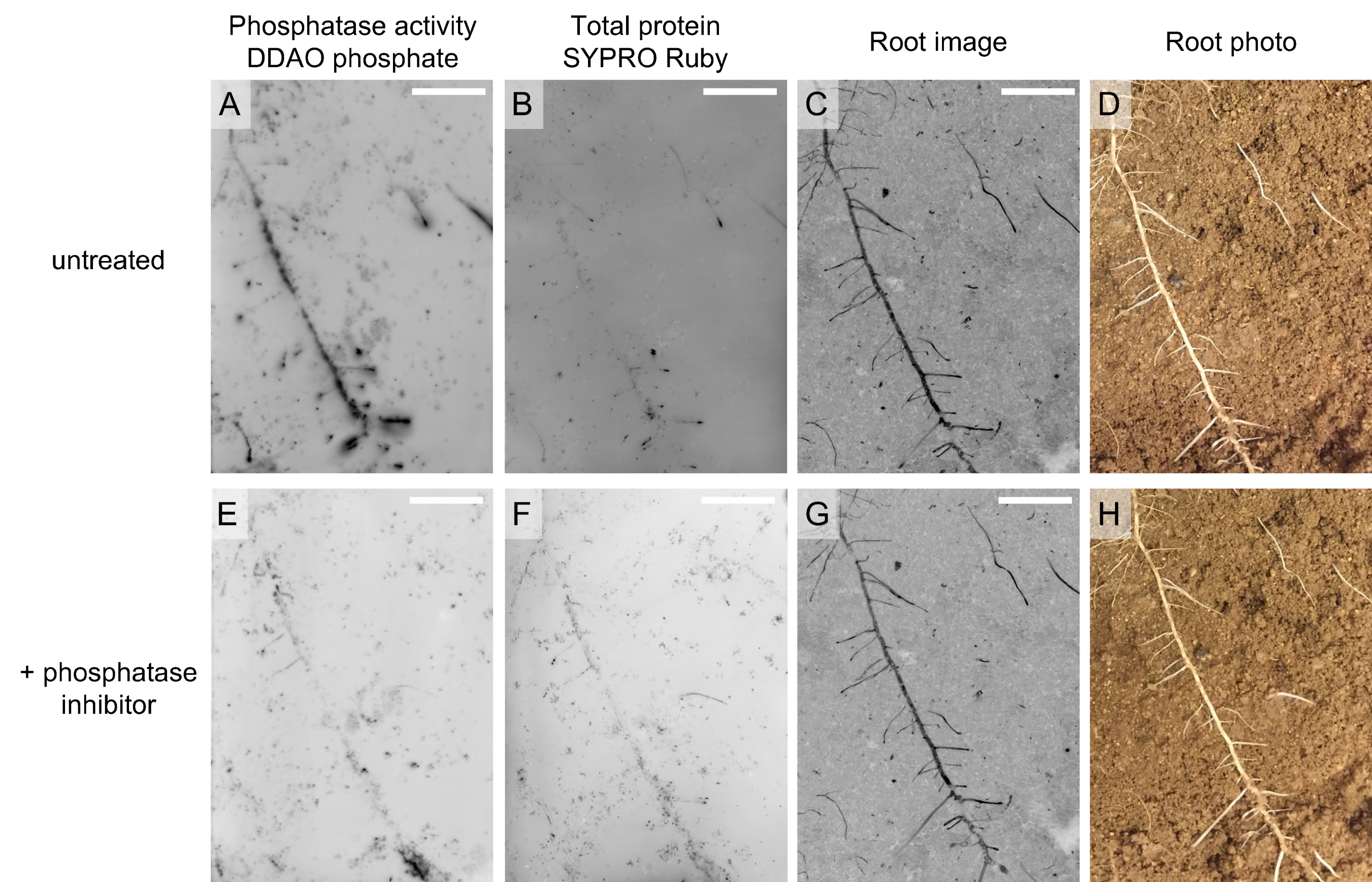


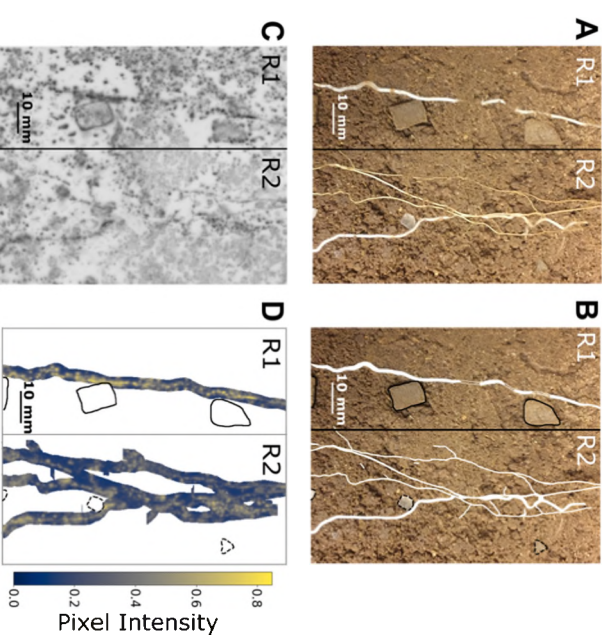


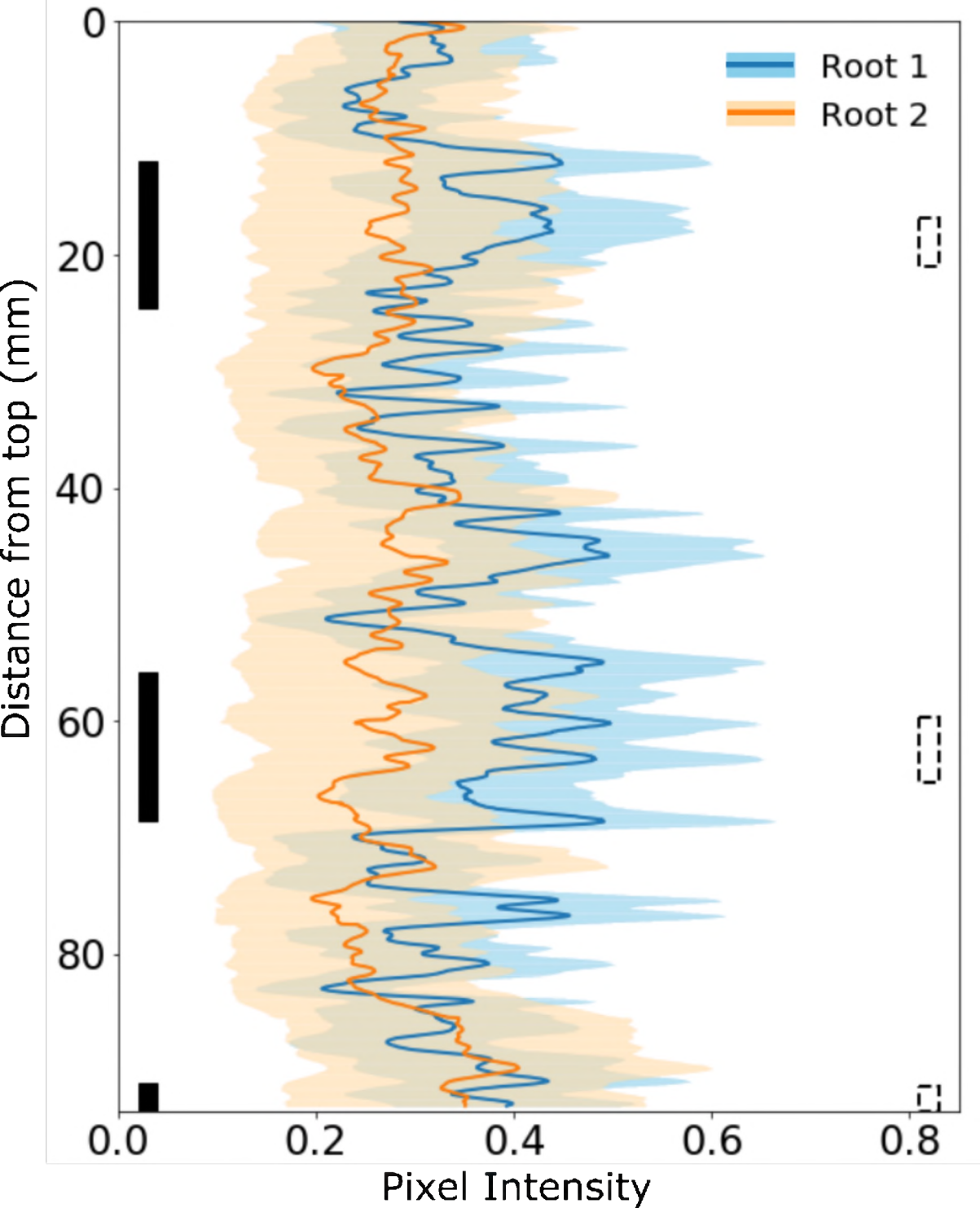












### **Highlights:**

- Method enables mapping of rhizosphere phosphatase and total protein distribution
- Non-destructive and can be used for timeseries analysis
- Identified hotspots of activity when combined with quantitative image analysis

Declaration of interests	
oxtimes The authors declare that they have no known competing financial interests or personal relationships that could have appeared to influence the work reported in this paper.	
□The authors declare the following financial interests/personal relationships which may be considered as potential competing interests:	
	_